From quantum glass to addressable spin clusters in the model magnet $\mathbf{LiHo}_x\mathbf{Y}_{1-x}\mathbf{F}_4$

by

Tatjana Hählen

Supervisor: Henrik Ronnow
Co-Supervisor: Ivica Zivkovic

Research Project, Semester 1
Master of Physics at EPFL

January 11, 2008

Abstract

This report describes an AC-susceptibility study on $LiHo_xY_{1-x}F_4$. $LiHo_xY_{1-x}F_4$ has different phases depending on the concentration x of holmium. Pure $LiHoF_4$ is a ferromagnet, at concentrations of $x \sim 0.20$ it is a spin glass and at concentrations of $x \sim 0.05$ it becomes a spin liquid. The crystal studied here is $LiHo_{0.04}Y_{0.96}F_4$. In this spin liquid phase it shows several interesting properties which differ from ordinary spin glasses. Its spectral width of the imaginary part of the magnetic susceptibility χ'' narrows with decreasing temperature contrary to spin glasses. We measured the real χ' and the imaginary part χ'' of the magnetic susceptibility at different temperature and over a frequency range of 5 decades. The data are an extension to higher temperature of already existing data and match well with them in the overlapping temperatures. Our data shows well the trend the shift of the peak of the response function for χ'' to higher frequencies and the decrease of the peak amplitude with increasing temperature. Also the cut of frequency for χ' increases with temperature. This is in agreement with the existing data at lower temperature.

Contents

List of Figures

1 Introduction

The aim of the research project was to investigate $LiHo_xY_{1-x}F_4$. This crystal has special properties depending on the concentration of holmium. Pure $LiHoF_4$ is a ferromagnet. For low concentrations ($x \sim 0.20$) it becomes a spin glass and at even lower concentration ($x \sim 0.050$) it becomes a spin liquid [3]. The spin liquid phase shows an interesting behaviour different from a spin glass. Its spectral width of the imaginary part of the magnetic susceptibility χ'' is decreasing with decreasing temperature contrary to a spin glass. Another interesting property is that hole burning can be applied on the spin liquid [6]. As this system is still not fully understood, further investigations are necessarily. The crystal used for our experiments was $LiHo_{0.04}Y_{0.96}F_4$.

2 Spin Glass

A spin glass is a magnetic system which has no long-range order as in a ferro- or antiferromagnetic system. It is characterized by random interactions and order. J.A. Mydosh defines a spin glass as following:

> "A spin glass is a random, mixed-interaction, magnetic system characterized by a random, yet co-operative, freezing of spins at a well-defined temperature T_f below which a highly irreversible, metastable frozen state occurs without the usual long-range spatial magnetic order." [1]

To get a spin glass two prerequisites are necessary. On the first hand either randomness in position of the spins or in the signs of the neighbouring couplings (ferro- ($\uparrow\uparrow$) or antiferromagnetic ($\uparrow\downarrow$)) is needed. Otherwise the system will be of a long-range ordered ferro- or antiferromagnetic state. On the other hand frustration of the spins is necessary. Because of the competing interactions spins are in a situation in which they can not satisfy all couplings. An example for a frustrated system is a triangular lattice with antiferromagnetic coupling (Fig. 1). The randomness can mainly be created in two different ways. One is the random-site occupancy in which the magnetic spins are distributed randomly in the crystal. This can be obtained by diluting a magnetic system. For this the magnetic element has to be replaced by a non-magnetic one. The other possibility is the bond-randomness. In this type of system the interaction varies randomly between ferro- and antiferromagnetic coupling.

At $T \to \infty$ a spin glass will be just a paramagnet. When the temperature is lowered the spins will group into clusters which then can rotate as a whole. As $T \to T_f$ the various spin components begin to interact with each other over a longer range, because the temperature disorder is being removed. The

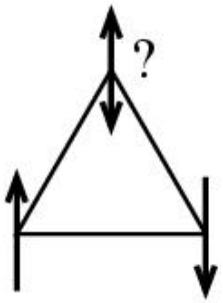

Figure 1: The antiferromagnetic coupling in the triangular lattice leads to frustration of the upper spin

system seeks its ground-state ($T = 0$) configuration. But partly because of frustration there is a set of ground states for the system to choose from. As there are lots of closely spaced energy levels with high barriers in between, the system may become trapped in a metastable configuration of higher energy. [1] Consequently, glasses have very slow relaxations, with a very broad distribution of relaxation times. [2]

3 $\mathbf{LiHo_xY_{1-x}F_4}$

3.1 General Properties of $\mathbf{LiHo_xY_{1-x}F_4}$

$LiHo_xY_{1-x}F_4$ is a model Ising magnet. The magnetic ion concentration is given by the concentration x of the Holmium spins. It exhibits a body centered tetragonal structure with four formula units in each unit cell, as shown in Fig. 2. Because of the crystal field anisotropy, the spin alignment is along the c axis making it an Ising magnet. As the system is insulating, conduction electrons play no role. The dominant coupling is the dipolar interaction. The dipolar interaction takes the form [1]:

$$\mathcal{H}_{ij}^{dip} = \frac{1}{r_{ij}^3}[\boldsymbol{\mu_i} \cdot \boldsymbol{\mu_j} - 3(\boldsymbol{\mu_i} \cdot \hat{r}_{ij})(\boldsymbol{\mu_j} \cdot \hat{r}_{ij})] \tag{1}$$

There is also a nearest-neighbour antiferromagnetic exchange coupling of 0.34 K. Since the dipolar interaction is weak and long ranged, the undiluted compound is a mean field ferromagnet with $T_c = 1.53$ K. When in $LiHo_xY_{1-x}F_4$ the magnetic Ho^{3+} ions are randomly substituted by Y^{3+}, the fact that the anisotropic dipolar interaction can be antiferromagnetic as well as ferromagnetic begins to matter. In fact the dipolar coupling is ferromagnetic for nearest neighbours and antiferromagnetic for next nearest neighbours. So by substituting randomly non magnetic Y^{3+} ions, the sign

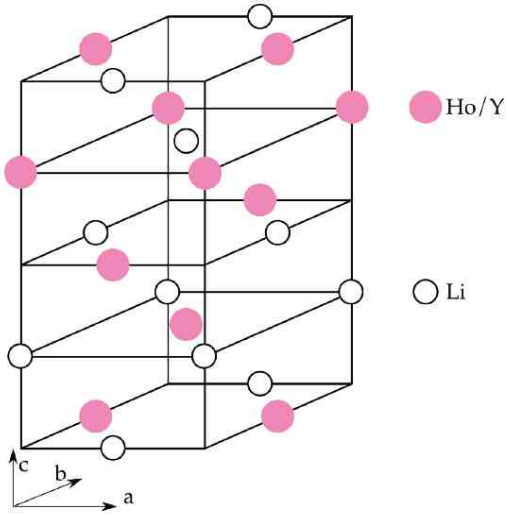

Figure 2: Unit cell of $LiHo_xY_{1-x}F_4$ showing the positions of the Holmium or Yttrium ions and the Lithium ions. [2]

and strength of the interaction become increasingly random. This leads to frustration in the system as the magnetic concentration x decreases. So the system freezes into a spin glass, as for the concentration of $x = 16.7\%$ and $x = 19.8\%$ [2]. However if $LiHo_xY_{1-x}F_4$ is further diluted by Y, the system shows non-glassy properties, also called "spin liquid". In this state there are only short range spin correlations which don't exceed a few unit cells and the spins continue to fluctuate as $T \to 0$. There are three possible reasons for a non-freezing of the spins; low-dimensionality, geometric frustration and zero-point quantum fluctuations. For $LiHo_xY_{1-x}F_4$ it is due to quantum fluctuations. The phase diagramm of $LiHo_xY_{1-x}F_4$ is shown in figure 3. [2, 3]

3.2 Unglassy behaviour of $LiHo_{0.045}Y_{0.955}F_4$

Differences of $LiHo_{0.045}Y_{0.955}F_4$ to an ordinary spin glass can be seen in its magnetic susceptibility, $\chi(f) = \chi'(f) + i\chi''(f)$. Ordinary disordered magnets respond to a changing external field via exponential relaxation $e^{-t/\tau}$, where τ is a characteristic time. In the frequency domain the susceptibility takes the Debye form:

$$\chi(f) = \frac{\chi_o}{1 + 2if\pi\tau} \tag{2}$$

The imaginary part $\chi''(f)$ has a smooth peak at $2f\pi\tau = 1$ and a full width at half maximum (FWHM) of 1.14 decades on a $\log_{10}$ frequency scale. Typ-

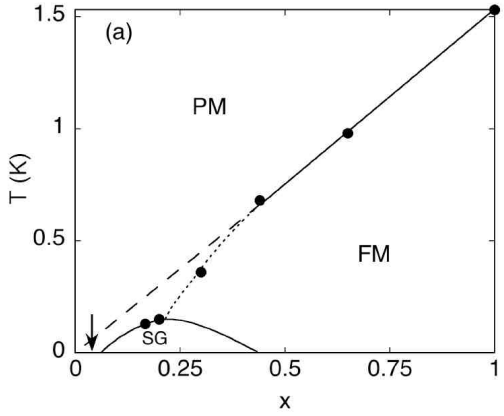

Figure 3: (Reproduced from [2]) Phase diagram for $LiHo_xY_{1-x}F_4$. PM=Paramagnet, FM=Ferromagnet, SG=Spin Glass. The arrow indicates the spin liquid phase.

ically there is a distribution of relaxation times in glasses and therefore the response function is a superposition of Debye forms for all the times τ in the distribution. Therefore $\chi''(f)$ is broader than the Debye form. The spectrum becomes progressively broader on cooling as the number of states in which the system can be trapped for long periods grows with decreasing T [3]. The peak will move to lower frequencies as the temperature is reduced because the characteristic times increase in general which corresponds to lower frequencies. For $LiHo_{0.045}Y_{0.955}F_4$ the spectral response actually narrows with decreasing temperature instead of the expected broadening for a glass (Figure 4). In the low temperature spin liquid phase of $LiHo_{0.045}Y_{0.955}F_4$ it becomes even narrower than Debye (0.8 decades at $T = 0.05$ K). Therefore classical relaxation of spins and spin clusters cannot describe the system. It can be also seen that the spectral response moves to lower frequencies with decreasing T as the spin relaxation becomes slower. Also the distribution becomes truncated at low frequencies [3, 4, 5, 6]. Figure 5 compares the imaginary part of the susceptibility χ'' of $LiHo_xY_{1-x}F_4$ for the spin glass ($x = 0.167$) and the spin liquid ($x = 0.045$).

3.3 Hole burning in $LiHo_{0.045}Y_{0.955}F_4$

The fact that the response function is narrower than Debye might be explained by a superposition of several sharp and narrow peaks instead of the glassy relaxation [3]. This would then be similar to a set of harmonic oscillators. So these oscillators should be addressable separately, which can be tested by hole burning.
Hole burning consists of exciting some of the oscillators at their resonance

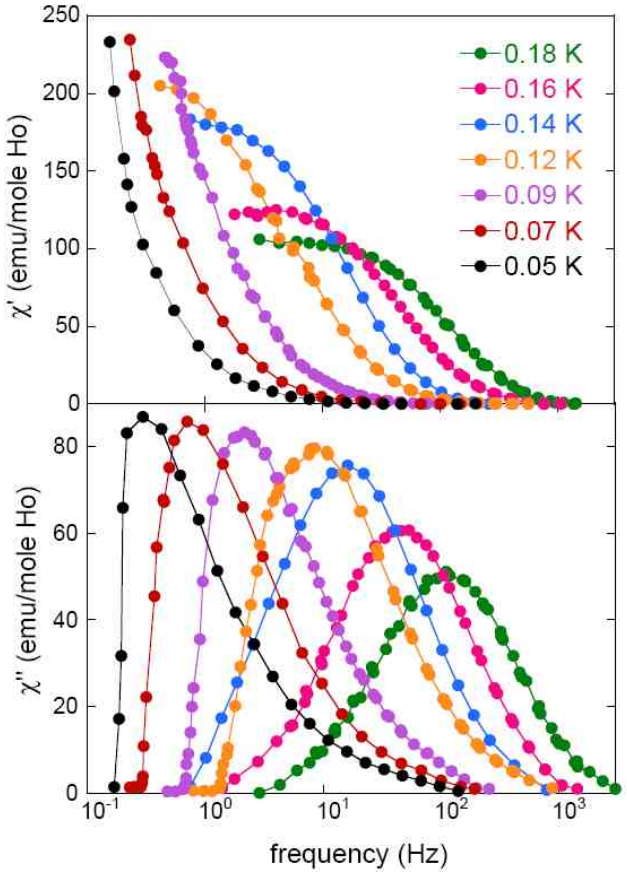

Figure 4: (Reproduced from [3]) Real (χ') and imaginary (χ'') parts of the magnetic susceptibility for $LiHo_{0.045}Y_{0.955}F_4$. The peak moves to lower frequencies with decreasing temperatures and the spectral width narrows.

frequency which leads then to a bleaching in the system response at that frequency.
By applying a fixed pumping frequency while measuring the spectrum with a small prob frequency, the hole burning can be tested.

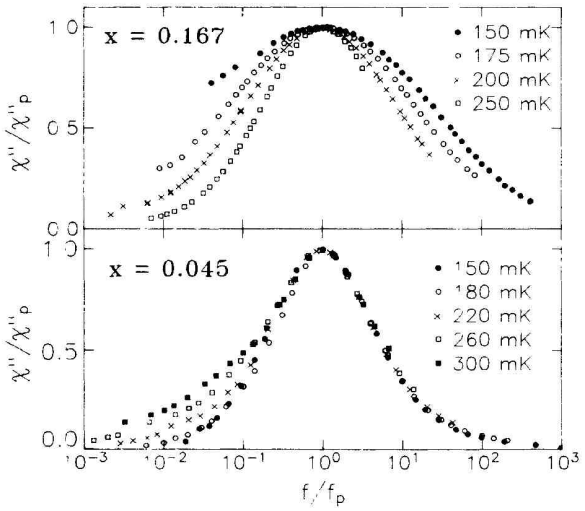

Figure 5: (Reproduced from [5]) Comparison of the imaginary parts of the magnetic susceptibility (χ'') , scaled by peak frequency and amplitude, for $LiHo_xY_{1-x}F_4$ for $x = 0.167$ (spin glass) and $x = 0.045$ (spin liquid). For the spin glass ($x = 0.167$) χ'' broadens with decreasing temperature, whereas it narrows for the spin liquid ($x = 0.045$).

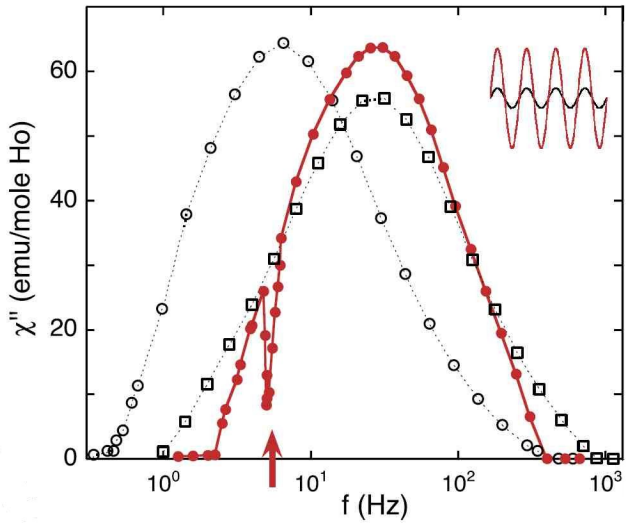

Figure 6: (Reproduced from [6]) Here the effects of applying a 0.2-Oe pumping frequency at $f = 5$ Hz are shown. The open black circles and the red circles show the imaginary part of the magnetic susceptibility χ'' at $T = 0.110$ K without and with pumping frequency respectively. The black open squares show χ'' at $T = 0.150$ K for comparison.

Figure 6 shows the different effects on the imaginary part of the magnetic susceptibility when a pumping frequency is applied. First it can be seen that the peak shifts from 6 to 27 Hz. Further it can be seen that the spectrum narrows above the peak. If the result is compared to the spectrum at $T = 0.150$ K which has the same peak frequency, it can be seen that the hole-burned spectrum is significantly narrower. The pump is therefore not simply heating the sample. Most importantly however is the hole burned at the pumping frequency of 5 Hz. A pump amplitude of 0.2 Oe (versus a probe amplitude of $h_{ac} = 0.04$ Oe) removes 75% of the original signal. The decay times of these oscillations have been found to rise from 4 to 10 s on cooling from 0.125 to 0.070 K [6].

4 Experimental Setup

In this Chapter some of the experimental techniques used for our experiments are explained.

4.1 ^{3}He-^{4}He-Dilution Refrigerator

To reach temperatures as low as 50 mK needed for our experiments, we used a ^{3}He-^{4}He dilution refrigerator. A dilution refrigerator exploits that at sufficiently low temperatures a mixture of ^{3}He and ^{4}He undergoes a phase separation into a ^{3}He and a ^{4}He-rich phase (Figure 7). When the temperature approaches $T = 0$, the ^{3}He-rich phase becomes pure ^{3}He, whereas the ^{4}He-rich phase has even at zero temperature a concentration of 6.5% ^{3}He in ^{4}He [7]. If the ^{3}He in the the ^{4}He-rich phase is reduced, ^{3}He-atoms will pass from the ^{3}He-rich phase to the ^{4}He-rich phase. During this transfer the system is cooled. To remove ^{3}He atoms of the ^{4}He-rich phase, a circuit as illustrated in figure 8 is used. The ^{4}He-rich phase is connected to the still we are pumping. As ^{3}He has a much higher vapour pressure than ^{4}He, mostly ^{3}He is pumped away ($> 90\%$). The concentration in ^{3}He in the still is then reduced and because of the osmotic pressure, ^{3}He atoms from the mixing chamber will move to the still. The ^{3}He atoms following from the ^{3}He-rich phase will then cool the system. As the ^{3}He is pumped by a pump at room temperature is has to be precooled and liquified before coming back to the ^{3}He-rich phase in the mixing chamber. This is done by several heat exchangers on the ways down. So the liquid from the mixing chamber going up to the still cools the down-coming ^{3}He from the pump. Before it passes by the 1K-pot (at 1.5 K). The 1K-pot consists of liquid ^{4}He which reaches a temperature of about 1.5 K by pumping on it [7].
The whole system sits in a vacuum chamber which is surrounded by liquid helium. This liquid ^{4}He bath also provides helium to the 1K-pot through a needle-valve.

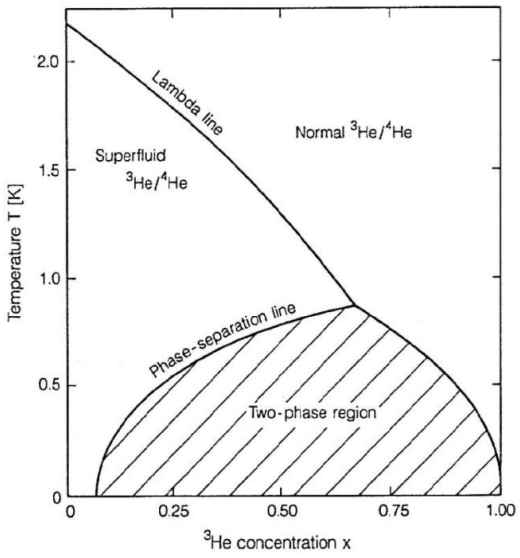

Figure 7: (Reproduced from [8]) Phase diagram of liquid ^{3}He-^{4}He mixtures at saturated vapour pressure. It shows the lambda line for the superfluid transition of ^{4}He. At low temperatures the mixture separates into a ^{3}He and a ^{4}He-rich phase. The shaded region corresponds to forbidden states.

4.2 Magnetic Susceptibility Measurement

The magnetic susceptibility is defined by $\chi = \frac{\mathrm{d}M}{\mathrm{d}h}$, where M is the magnetization and h an applied magnetic field. For small magnetic fields, the magnetization is proportional to the magnetic field and the magnetic susceptibility becomes therefore simply $\chi = \frac{M}{h}$. This is also called the linear regime. To measure the magnetic susceptibility we use three coils wounded in a concentric manner. One of them are the excitation coils on which an *ac* current is applied. This then creates a magnetic field which induces a magnetization M in the crystal. The other two are the pick-up coils. One of them detects the induced magnetization through induction and the other one is used to cancel the mutual inductance. The excitation coils create a magnetic field of $h_{ac} = 4\pi nI/c$, with n the number of turns per unit length, I the excitation current and c the speed of light. The susceptibility at a frequency ω can then be calculated from the induced voltage V by,

$$\chi = \frac{Vc^2}{16\pi^2 \mathrm{i}\omega I_o n N F A}, \tag{3}$$

where I_o is the amplitude of the current, N and A the number of turns and the area of the pick-up coils, respectively. f is the filling factor and defined as the fraction of the volume of the coils occupied be the crystal [2]. The total voltage in the pick-up coils comes from the sample inductance and from

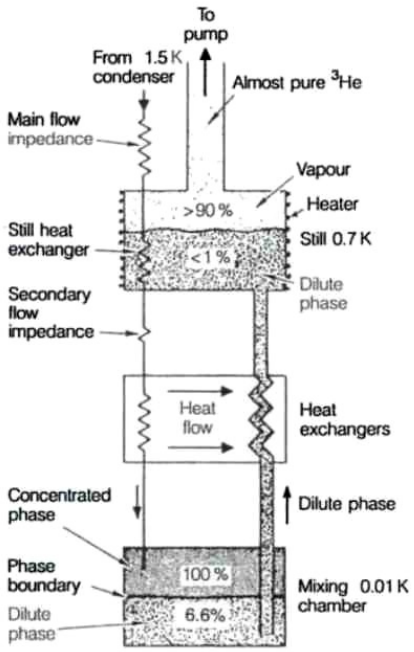

Figure 8: (Reproduced from [7]) Schema of a ^{3}He-^{4}He dilution refrigerator

the mutual inductance. The sample inductance of the two coils differs due to their different filling factor. The mutual inductance of the two coils should be identical. In reality this is not the case and gives therefore a background. The voltage finally measured is the substraction of the induced voltages in the two coils.
For our measurements we just used the relation of the magnetic susceptibility to the applied current, the measured voltage and the frequency ν:

$$\chi \propto \frac{V}{I\nu} \tag{4}$$

For our experiments, the set-up as illustrated in figure 9 has been used. The crystal is placed within the coils so that the induced magnetic field is parallel to the Ising axis. The read-out coils were directly connected to the lock-in amplifier. To get the real and the imaginary part of the magnetic susceptibility $\chi = \chi' + \mathrm{i}\chi''$, a reference phase is needed. This one is set by the resistance $R_{meas} = 1\Omega$. As we don't use an additional current limiting resistance, the current and therefore the induced magnetic field varies with frequency for the same applied voltage. Because the induced magnetic field should be constant for all frequencies, the voltage has to be varied so that a field of 0.1 Oe is induced from the exciting coils for all frequencies.

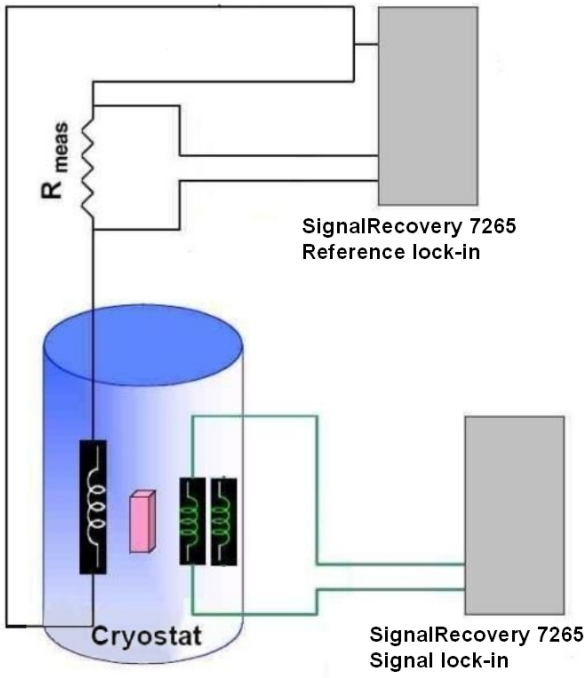

Figure 9: Schema of the electronic set-up. R_{meas} is set to 1 Ω and the voltage is varied in order to have a induced field of 0.1 Oe for all frequencies.

The susceptometer used is one produced commercially by CMR. The coils consist of copper wires of a thickness of 25 μm and a total thickness with insulation of 36 μm. The inner pick-up coils (P1) have an inner diameter of 2.6 mm, an outer diameter of 3.8 mm and 5272 turns. The outer pick-up coils (P2) have an inner diameter of 3.8 mm, and outer diameter of 4.5 mm and 2974 turns. The exciting coils have an inner diameter of 4.5 mm, an outer diameter of 5.6 mm and 3867 turns. All coils have a length of 10 mm. The coils are connected so that there is access to the excitation coils as well as the difference of the two pick-up coils (P1-P2), which gives the magnetization. The expected induced field is of 4.2 Gauss/mA.

4.3 Lock-in Amplifier

The lock-in amplifier we used for our experiments was a SignalRecovery 7265. A lock-in amplifier is used to extract the signal at a known frequency from the noise. The signal can be extracted by comparing it to a reference signal of the same frequency as the signal to be measured. This is done in mainly four stages [9]:

- *Input Gain Stage*
  It is used to amplify the signal to a level suitable for the demodulator.

- *Reference Circuit*
  It allows to phase shift the reference signal.

- *Demodulator*
  It multiplies the reference and the input signal together. Supposing the two signals are sinusoidal, we get

$$V_{sig}\sin(\omega_{sig}t+\phi_{sig})\cdot V_{ref}\sin(\omega_{ref}t+\phi_{ref}) = \tag{5}$$
$$\frac{1}{2}V_{sig}V_{ref}\left\{\cos\left[(\omega_{sig}+\omega_{ref})t+\phi_{sig}+\phi_{ref}\right]+\cos\left[(\omega_{sig}-\omega_{ref})t+\phi_{sig}-\phi_{ref}\right]\right\}.$$

  As the signal to be measured and the reference signal have the same frequency, the frequency difference is zero.

- *Low Pass Filter*
  It will remove the AC signals. So the first cosin with the sum of the frequencies will be removed. Also the second cosin will be removed unless the two frequencies are equal. Therefore only the part of the signal having the same frequency as the reference will be left. The output will be

$$\frac{1}{2}V_{sig}V_{ref}\cos\left(\phi_{sig}-\phi_{ref}\right). \tag{6}$$

  So the input signal has been transformed in a DC signal proportional to the signal amplitude. If the reference phase is set equal to the phase of the signal, the output is just $\frac{1}{2}V_{sig}V_{ref}$ however if the phase difference is 90° the output is zero. This phase dependency can be eliminated by a second reference signal of $V_{ref}\sin(\phi_{sig}+\frac{\pi}{2})$. In this case the output is

$$\frac{1}{2}V_{sig}V_{ref}\cos\left(\phi_{sig}-\phi_{ref}+\frac{\pi}{2}\right)=\frac{1}{2}V_{sig}V_{ref}\sin\left(\phi_{sig}-\phi_{ref}\right). \tag{7}$$

  So two outputs X and Y can be extracted:

$$X = V_{sig}\cos(\phi) \tag{8}$$
$$Y = V_{sig}\sin(\phi), \tag{9}$$

  where ϕ is the phase difference $\phi_{sig}-\phi_{ref}$ [10].

4.4 Sample Mounting

The measured crystal is $LiHo_{0.04}Y_{0.96}F_4$ and has the approximative size of $10\times 1\times 0.5$ mm^3. A big problem for the measurements was to control the

temperature of the sample itself and to guaranty ist stability. Using a RuO_2 thin film resistor next to the sample allows to monitor the temperature. Additional copper wires were then wrapped around the sample allowed then a better heat conductance (figure 10). This is needed as otherwise the heat conductance in the milli-Kelvin range is too low otherwise. To avoid skin effects, these wires have to be very thin. The hole system sits on a sapphire stick and is then put into stycast to insure the stability of the system.

Figure 10: Here a schema of the sample mounting is shown. The resistor (black) sits behind the $LiHo_{0.04}Y_{0.96}F_4$-crystal. The Cu-wire insures a good thermal conductance. The whole system is then put into stycast.

5 Results

The susceptibility measurements have been done with the method described above on $LiHo_{0.04}Y_{0.96}F_4$. To get an additional temperature monitoring, a thin film resistor of RuO_2 has been placed next to the sample. The RuO_2 resistor has a resistance of 1 kΩ at room temperature. For temperatures below 1 K the resistance is increasing which allows relatively good temperature sensitivity. The stability of the temperature of the sample itself can therefore be well monitored.
The results of the real (χ') and imaginary part (χ'') of the magnetic susceptibility over five decades of frequency and for different temperatures can be seen in figure 11. For each frequency several measurements have been taken. The data points correspond to the median of the measured susceptibilities at a given frequency. The error bar is calculated using the standard deviation.

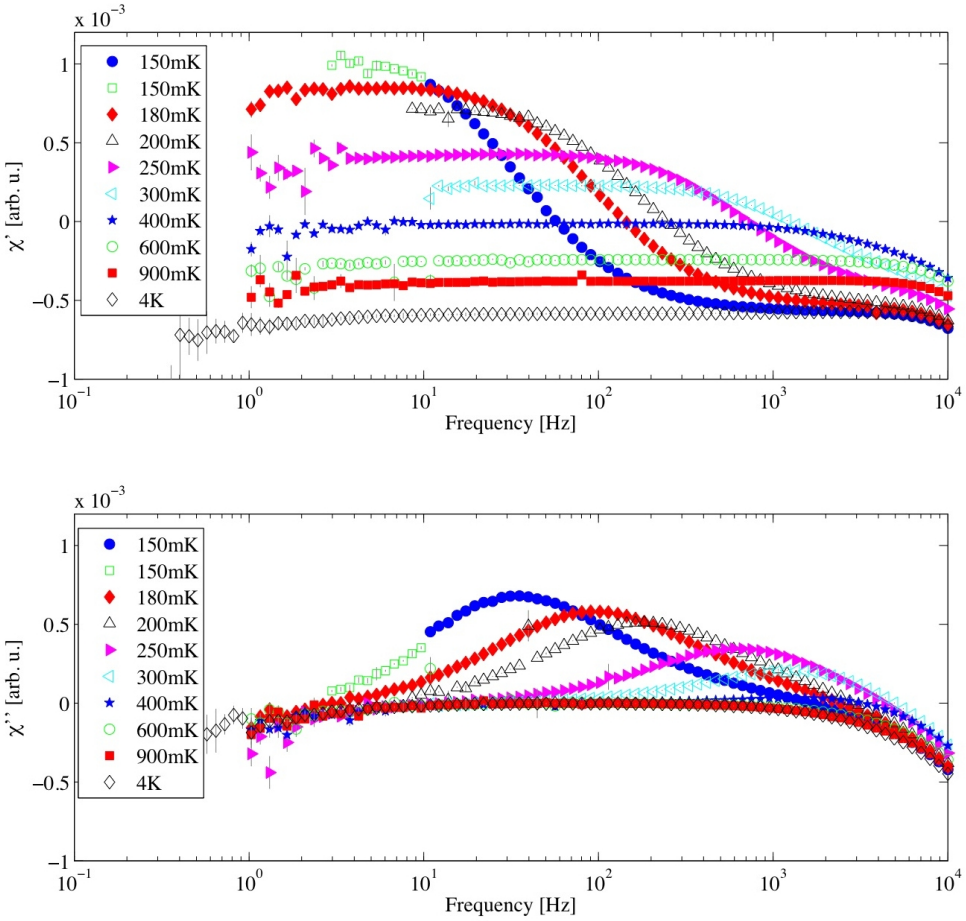

Figure 11: Here the results of the real (χ') and the imaginary part (χ'') of the magnetic susceptibility are presented. The results at 4 K correspond to the background.

From the result at 4 K it can be clearly seen that there is some background. At 4 K the imaginary part of the susceptibility should be zero at all frequencies. It can also be seen that the other values are approaching the curve at 4 K and for the imaginary part there is almost no difference between the curve at 4 K and the one at 0.9 K. So to remove the effects of the background, we subtracted the results at 4 K from the measured results at lower temperatures. As the real part of the magnetic susceptibility is not necessarily zero, there might be a slight shift. We get then the results as illustrated in figure 12 after subtracting the background.

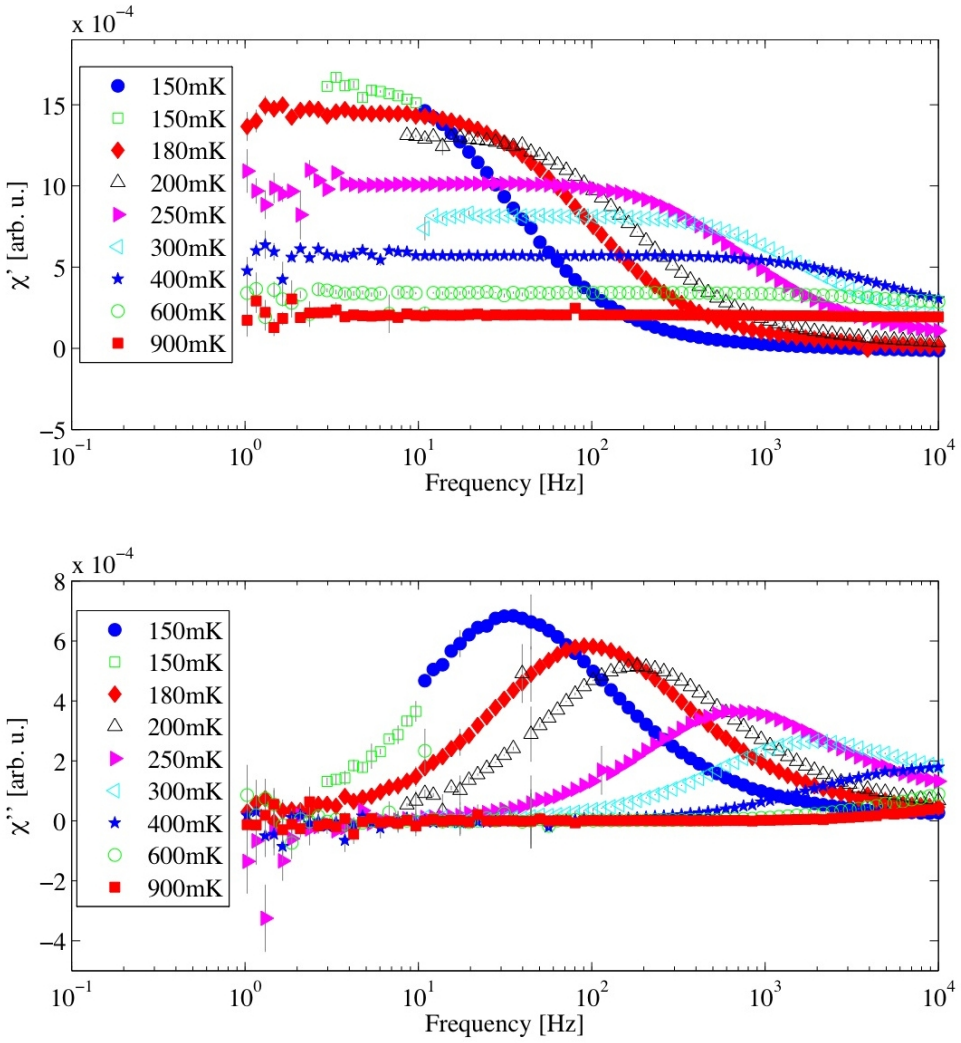

Figure 12: Here the results of the real (χ') and the imaginary part (χ'') of the magnetic susceptibility after subtracting the background are presented.

There are several effects that can been seen on figure 12. For the real part of the magnetic susceptibility (χ') it can be seen on one hand that the cut-off frequency goes to higher frequencies as the temperature is raised. On the other hand the the amplitude is reduced with increasing temperature (see also figure 13). For the imaginary part of the magnetic susceptibility (χ'') it can be seen that the peak is shifted to higher frequencies and that the peak size is decreasing with higher temperatures (see also figure 14 and 15). If the FWHM is decreasing with decreasing temperature can not be clearly seen however it seems as this would be the case.

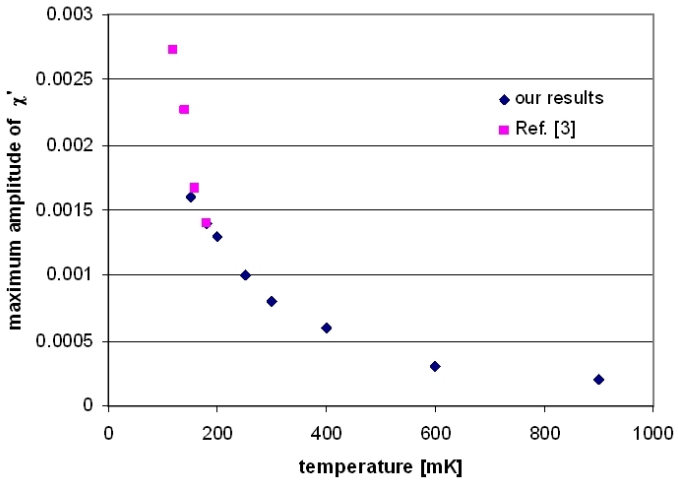

Figure 13: The evolution of the maximum amplitude of the real part of the magnetic susceptibility χ' is shown. For comparison also the data from Ref. [3] has been placed (scaled to our results). The two datas match well together. The maximal amplitude follows a potential law.

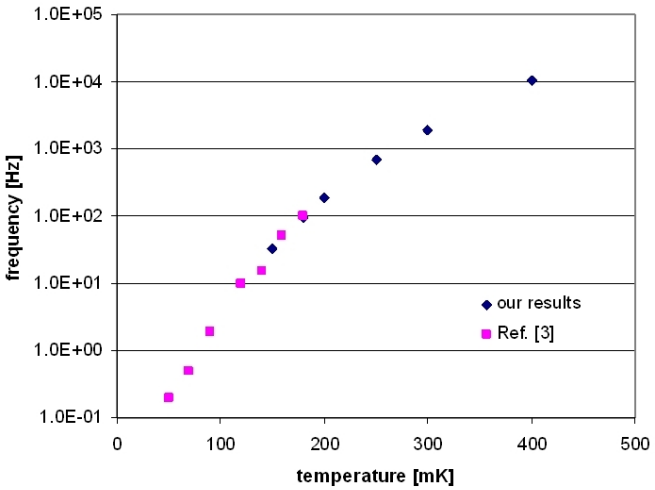

Figure 14: The evolution with temperature of the peak frequency of the imaginary part of the magnetic susceptibility χ'' is shown. For comparison also the data from Ref. [3] has been placed. The two datas match well together. It can be seen that the peak frequency grows less than exponentially with temperature.

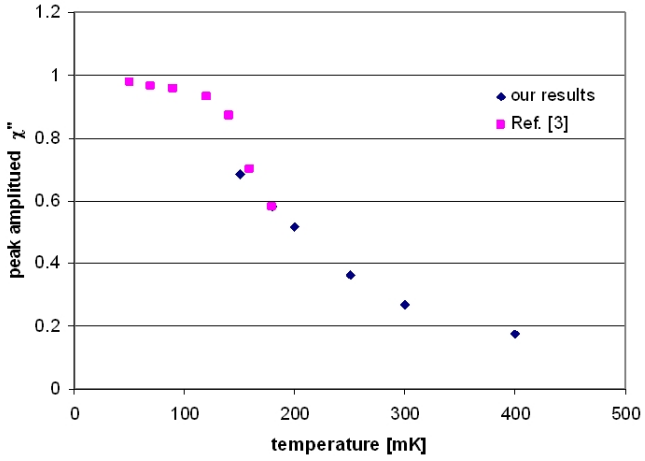

Figure 15: The evolution with temperature of the peak amplitude of the imaginary part of the magnetic susceptibility χ'' is shown. For comparison also the data from Ref. [3] has been placed (scaled to our results). The amplitude seems to approach a finit value at zero temperature.

Another interesting point is that the peak of χ'' and the inflection point

of χ' are at the same frequency. This is illustrated in figure 16. Here the imaginary part of the magnetic susceptibility χ'' and the derivative of the real part of the magnetic susceptibility versus the logarithm of the frequency, $\frac{d\chi'}{d(\log(\nu))}$ is shown. It can be seen that the two curves peak at the same frequencies for the three temperatures.

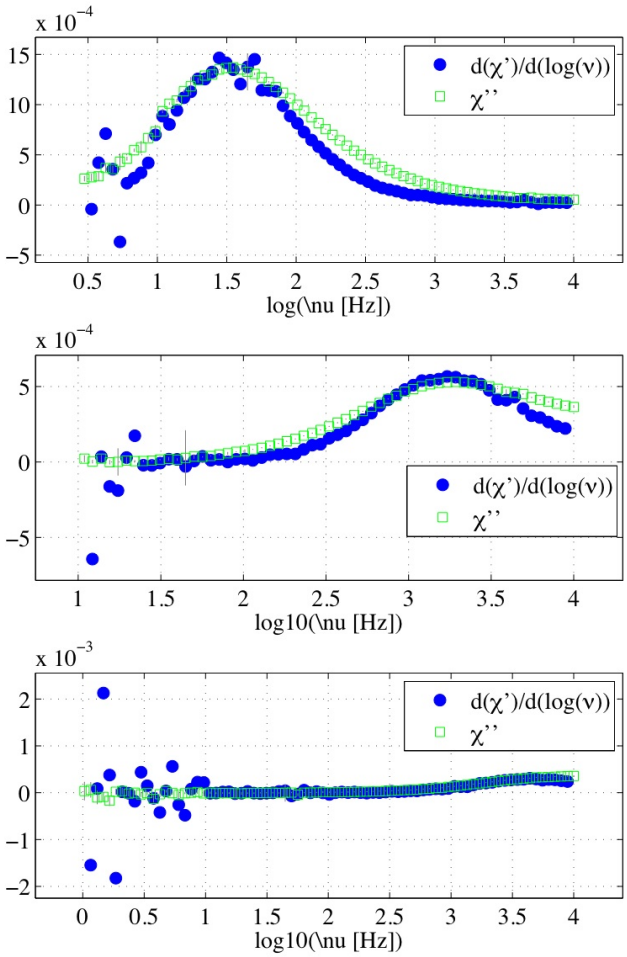

Figure 16: To compare the peak of χ'' and the inflection point of χ', χ'' and $\frac{d\chi'}{d(\log(\nu))}$ are drawn for three different temperatures (T=150 K, 300 K and 400 K respectively). It can be seen that the derivative peaks at the same frequency as χ''.

6 Conclusion

We measured the AC-susceptibility of $LiHo_{0.04}Y_{0.96}F_4$ over 5 decades in frequency and for different temperatures between 150 mK and 900 mK. We were able to reproduce the data from Ref. [3] in the temperature range between 150 mK and 180 mK and got more data for higher temperatures. The data shows that the cut-off frequency of the real part of the magnetic susceptibility moves to higher frequencies with increasing temperature. The peak of the imaginary part of the magnetic susceptibility is shifted to higher frequencies and decreases in amplitude as the temperatures is increased. This observations are in good agreement with Ref. [3]. At low frequencies the noise was unfortunately bigger than the signal. Therefore we were unable to get accurate data at lower temperatures as there the spectral response is at lower frequency.
Next thing to do would then be to control better the noise at lower frequencies to investigate the magnetic susceptibility at lower temperatures. Later on the hole burning should be investigated to understand better this process.

7 Acknowledgements

I would like to thank Henrik Ronnow and Ivica Zivkovic for the time they took to explain me the phenomena of a spin glass and where $LiHo_{0.04}Y_{0.96}F_4$ shows its different behaviour. Before I only heard about the term "spin glass" but had no idea about its nature.

References

[1] J.A. Mydosh, *Spin Glasses: An Experimental Introduction*, Taylor & Francis

[2] Carlos. E. Ancona-Torres, *Relaxation in Quantum Glasses*, Ph.D. thesis, Department of Physis, The University of Chicago, Illinois, 2007

[3] Sayantani Ghosh, *Non-linear Dynamics in Spin Liquids*, Ph.D. thesis, Department of Physis, The University of Chicago, Illinois, 2003

[4] D.H. Reich, T.F. Rosenbaum, *Glassy Relaxation without Freezing in a Random dipolar-Coupled Ising Magnet*, Phys. Rev. Lett., 1987

[5] D.H. Reich, B. Ellman, J. Yang, T.F. Rosenbaum, *Dipolar magnets and glasses: Neutron-scattering, dynamical, and calorimetric studies of randomly distributed Ising spins*, Phys. Rev. B, 1990

[6] S. Ghosh, R. Parthasarathy, T.F. Rosenbaum, G. Aeppli, *Coherent Spin Oscillations in a Disordered Magnet*, Science, 2002

[7] Frank Pobell, *Matter and Methods at Low Temperatures*, Springer-Verlag, Berlin

[8] Image source: http://www.cresst.de/bigpic_refrigerator1.php

[9] Boston Electronics: http://www.boselec.com/products/siglimwhat.shtml

[10] About Lock-in Amplifiers: http://www.cpm.uncc.edu/programs/lia.pdf